Security engineering problems: determination of tolerance intervals for azimuthal positional errors

Ján Ivanka, Vladimíra Osadská

INSIGHTS INTO REGIONAL DEVELOPMENT
ISSN 2669-0195 (online) http://jssidoi.org/IRD/
2022 Volume 4 Number 1 (March)
http://doi.org/10.9770/IRD.2022.4.1(7)

Publisher
http://jssidoi.org/esc/home

SECURITY ENGINEERING PROBLEMS: DETERMINATION OF TOLERANCE INTERVALS FOR AZIMUTHAL POSITIONAL ERRORS

Ján Ivanka [1], Vladimíra Osadská [2]

[1] *Department of Security Engineering, Tomas Bata University in Zlín, Czech Republic*
[2] *FBI - Faculty of Safety Engineering, VŠB-Technical University of Ostrava, Czech Republic*

E-mails:[1] *ivanka@utb.cz*; [2]*vladimira.osadska@vsb.cz*

Received 28 Janaury 2022; accepted 8 March 2022, published 30 March 2022

Abstract. The aim of the paper is to provide an overview of the advantages and disadvantages of near-zone measurements and a comparison of near-zone and far-zone measurements. The paper is intended for specialists who will solve quite different problems - programs for numerical calculation of the far-zone field, including probe correction, back projection and gain, software for displaying the calculated values, programs for controlling the sensing equipment and measuring instruments, hardware equipment and instruments for measurements, including the design of the sensing equipment. The paper gives an overall overview as far as possible in a way that is understandable to experts in different fields, as it is necessary for them to be able to interact with each other and use a common language. The paper gives an analysis of the tolerance requirements for the X-Y positioning mechanism (planar sensing). For any measurement technique, one of the basic requirements is a reliable estimation of the measurement errors, and this is especially true for methods that use a high level of mathematical analysis, such as near-zone antenna measurements. Determining error margins for any measurement system for a given antenna/probe/near-zone combination can be a difficult and time-consuming task, and mathematical complexity is a major reason for the difficulty.

Keywords: probe correction; main and lateral lobe; azimuthal characteristics; final sensing; error functions; laser interferometer; correlation function

Reference to this paper should be made as follows: Ivanka, J., Osadská. V. 2022. Security engineering problems: determination of tolerance intervals for azimuthal positional errors. *Insights into Regional Development*, 9(3), 105-115. http://doi.org/10.9770/IRD.2022.4.1(7)

JEL Classifications: J28

Additional disciplines: security engineering

1. Introduction

There is a separate strand of literature devoted to engineering security problems (e.g. (Ivanka, Chuda, 2015; Buday, Grinchuk, Gromyko, 2017, Prabhakaran, Selvadurai, 2018; Bayuk, 2021; Chou et al., 2021).

To determine the tolerance requirements with respect to the accuracy of the measurement mechanism in the antenna/probe/near-zone combination is a time-consuming task and the mathematical complexity is the main reason for the difficulty.

ISSN 2669-0195 (online) http://jssidoi.org/jesi/
2022 Volume 4 Number 1 (March)
http://doi.org/10.9770/IRD.2022.4.1(7)

Therefore, attempts are often made to circumvent mathematical methods and try to set error limits for a general measurement technique by measuring for a particular antenna. In this approach, the results of the far-zone and near-zone measurements are compared, and the differences between the two methods are taken as a measure of the error in the near-zone measurements. The limitations of this approach are as follows:

a) The observed differences are partly and perhaps mainly due to errors in the remote zone,

b) it is difficult to generalise one result to another antenna or measurement system,

c) the most critical measurement parameters or contributions from individual error sources cannot be determined,

d) remote zone measurements may be impractical for certain types of antennas that are suitable for measurement in the near zone.

This is not to say that such comparisons have no value. They demonstrate reliability, help to ensure credibility without detailed mathematical analysis, and show possible areas where more detailed analysis is needed. They are one part of the error analysis, but they certainly do not form the whole picture. A complete and general analysis requires a combination of different approaches, both analytical and experimental, to identify all possible sources of error and estimate their contributions to the final calculated results. Such an analysis provides a means for the systems engineer to determine the requirements for each part of the measurement system in the near zone and for measurement theory experts to estimatethe uncertainty in the measured quantities.

The prerequisite of the analysis is to determine all significant sources of error, measure or estimate all sources of measurement error in the near zone, and in many cases determine the shape of the functional dependence of the errors. The error equations between the measurement errors in the near zone and the results of the calculations for the far zone were derived. The combinations of the individual error components are identified to obtain a realistic estimate of the resulting measurement errors. Detailed theoretical relationships that are important for measurement refinement (finite-dimensional analysis of the sensing for cylindrical sensing and analysis of the accuracy of the sensing mechanism) are presented.

These relations form the basis for the analysis of the tolerance requirements for the positioning mechanism for cylindrical measurements with respect to the positioning mechanism accuracies (azimuth/elevation). The cylindrical sensing technique has probably attracted the least interest in error analysis of all the commonly used sensing techniques. It was generally assumed that the errors would be similar to those for planar surface measurements, which is of course true, but some sources of error that have different implications need to be investigated. Detailed analyses have shown that the main source of errors is due to the influence of the measurement system.

2. Basic Errors in the Measured Antenna Settings

For the following analysis, we consider the spherical (R, θ, φ) and cylindrical (r, φ, z) coordinate systems.

Typically, the axis of rotation (z-axis) will be vertical for scanning on a cylindrical surface. Errors in the alignment of the antenna being measured will cause the antenna coordinate system as defined by the mirror, base markers, or telescope to not be exactly aligned relative to the coordinate system of the scanning mechanism. Since the resulting characteristic is defined relative to the mechanical sensing plane, misalignment of the measured

ISSN 2669-0195 (online) http://jssidoi.org/jesi/
2022 Volume 4 Number 1 (March)
http://doi.org/10.9770/IRD.2022.4.1(7)

antenna will cause a maximum radiation error equal to the azimuthal and elevation rotation errors. A small misalignment will cause approximately equivalent azimuth and elevation errors that are not too far off axis.

The theoretical analysis for planar sensing in the x,y plane, as presented in (Rensburg et al., 2020; Just, 1981; Chejbal, Kovarik, 1981; Epjar et al., 1988; Newell, 1988; Newell, Lee, 2000; OHDE, 2007/2008) can be used to estimate the errors in the probe position in the z-axis direction. For the case where the main beam is approximately perpendicular to the z-axis, the errors for the gain maximum and side lobes are

$$\Delta G(\theta,\varphi)_{dB} \le \frac{8{,}7\Delta_z(\text{rms})}{\eta D_z} g(\theta,\varphi) \quad \text{for the main lobe,} \qquad (1)$$

$$\Delta P(\theta,\varphi)_{dB} \le \frac{4{,}3\Delta_z(\theta,\varphi)}{D_z} g(\theta,\varphi) \quad \text{for the lateral lobes,} \qquad (2)$$

Where:
G is the gain of the antenna,
P is the relative diagram, Dz is the principal dimension of the antenna,
η is the efficiency of the antenna aperture, and Δz is the position error in the z-axis.

The function $g(\theta,\varphi)$ is the ratio of the maximum of the diagram to the amplitude in the direction under consideration. For example, for a side lobe of -40 dB, $g(\theta,\varphi)$ is equal to 100. In equations (1) and (2), we consider the error spectrum for the angles (θ,φ). For the random error case, errors with the same rms value (standard deviation) are considered, which is emphasized by the rms notation. Considering the analysis, it is clear that all conclusions, which are related to in-plane sensing (x, y position error), including the examples given, apply analogously. If we know the error spectrum Δz-position, we obtain very realistic estimates of the near-zone errors. Upper bounds on the errors when we consider only the maximum value of the errors arise in rather special cases.

3. Radial and Azimuthal Positional Errors

The effect of the radius errors is similar to the z-direction position errors for planar sensing because these errors predominantly produce phase errors as a function of z and azimuth φ. For a fan-shaped measured antenna beam (narrow beam in the elevation plane and wide beam in the azimuthal plane) where the near-field phase is nearly constant on the cylindrical surface, the equations for the radius errors are identical to those for the z-direction position errors for planar sensing. For a pencil beam (a narrow beam for both azimuthal and levation planes), the magnitude of the phase for a given radius error varies with azimuth angle. This results in an approximate average phase error being considered in this case, cylindrical scanning. Therefore, as a result, we use the equations for planar scanning for a beam deflected 45° from the z-axis.

The mathematical relations for the main beam and side lobes of the pencil beam for the wavelength are λ:

$$\Delta G(\theta,\varphi)_{dB} \le \frac{22}{\sqrt{\eta}}\left(\frac{\delta_r(\text{rms})}{\lambda}\right)^2 g(\theta,\varphi) \quad \text{for the pencil main volume,} \qquad (3)$$

ISSN 2669-0195 (online) http://jssidoi.org/jesi/
2022 Volume 4 Number 1 (March)
http://doi.org/10.9770/IRD.2022.4.1(7)

$$\Delta P(\theta,\varphi)_{dB} \le \frac{10\delta_r(\theta,\varphi)}{\lambda} g(\theta,\varphi) \quad \text{for the side lobes of the pencil bundle.} \qquad (4)$$

In relations (3) and (4) we consider the error spectrum $\delta_r(\theta,\varphi)$. For the random error case, errors with the same rms value (standard deviation) are considered, which is emphasized by the notation rms. If we know the error spectrum $\delta_r(\theta,\varphi)$ of the z position, we obtain very realistic estimates of the errors in the near zone. Upper bounds on the errors, where we consider only the maximum value of the errors, arise in rather special cases.

The effect of azimuthal position errors can also be determined using a modified version of the equations for z-axis errors in planar sensing. The modification uses the y position errors that cause the azimuthal position errors. The y position when the probe moves azimuthally along the cylinder, where the differential of this position will give the corresponding error:

$$y = r\,[\cos(\varphi - 1)], \qquad \delta_y(\varphi) = r \sin(\varphi)\,\delta_\varphi. \qquad (5)$$

The y errors that have the greatest effect are the errors within the near-field collimation region. This region is practically equal to the aperture region of the measured antenna. For an antenna with an aperture width Dx in the x-direction, the collimation region on the cylindrical scanning surface is bounded approximately by the angles

$$\varphi_y = \pm \arcsin[D_x/(2r)]. \qquad (6)$$

Therefore, the error y will vary between zero when $\varphi = 0$ and the maximum

$$\delta_y(\varphi) = \pi D_x \delta_\varphi/360 \qquad (7)$$

for δ_φ in degrees. The average error y is equal to one half of the value in equation (7). To determine the effect of azimuthal positional errors we use equations (3) and (4) with this error:

$$\Delta G(\theta,\varphi)_{dB} \le \frac{22}{\sqrt{\eta}} \left(\frac{\pi D_x \delta_\varphi(\text{rms})}{180\lambda} \right)^2 g(\theta,\varphi) \qquad (8)$$

$$\Delta P(\theta,\varphi)_{dB} \le \frac{\pi D_x \delta_\varphi(\theta,\varphi)}{18\lambda} g(\theta,\varphi) \qquad (9)$$

Typical positional errors that can occur in cylindrical measurements are errors created by misalignment of the sensing mechanism on the straight line and the rotation axis of the antenna being measured. These errors can be estimated using relations (3) to (9). In addition to the radius errors, the actual alignment of the probe inside the measurement system in the near zone on the cylindrical surface is very important.Ideally, the x1 axis must be perpendicular to the z0 rotation axis and also intersect this axis.

Furthermore, the probe axis z1 must be parallel to the axis z0. It is well known from the theory of nearzone measurement on a plane that poor probe alignment translates directly to errors in the far zone, where the error is proportional to the change in probe characteristic. In the case of cylindrical sensing, this problem is somewhat more complicated and is presented in the area of measurement error analysis.

ISSN 2669-0195 (online) http://jssidoi.org/jesi/
2022 Volume 4 Number 1 (March)
http://doi.org/10.9770/IRD.2022.4.1(7)

In near-zone planar sensing, the antenna to be measured is mounted stationary and the near-zone probe moves along the planar surface in both the x and y directions so that the array of field patterns (amplitude and phase) can be sensed. Similarly, when scanning on a cylindrical surface, we scan the matrix of field samples for motion in the z-direction and in the azimuth φ. The scanning range for measurement in the z-direction is important when the accuracy of measurement on a cylindrical surface in the near zone is considered. The size of the antenna to be measured and the size and location of the final sensing area (cylinder) define the critical angle Φ. The calculated antenna radiation characteristics will be valid in the region between ±Φ. For a given sensing range L, the following applies:

$$L = D + P + 2d \text{ tg } \Phi, \quad (10)$$

Where:
D is the diameter of the measured antenna, P is the diameter of the probe and d is the distance between the probe and the measured antenna. Full angular coverage can only be achieved by sensing on the full spherical surface in the near zone. For example, a critical angle Φ= 70° is achieved with a scan that is six wavelengths on each side larger than the aperture of the antenna, two wavelengths away from the antenna.

The limited sensing area has two effects. First, for an area larger than the antenna aperture, the resulting radiation areas are only valid within the area. This criterion is used to determine the minimum scan plane dimension for a given desired angular area and separation distance d. Since the lower limit for d is determined by the physical structure of the antenna and multiple reflections, a trade-off is usually required between both maximum angular coverage along with error reduction due to limited scanning (when small d is required) and minimum multiple reflections (when large d is required).

Another effect of the limited sensing area is the occurrence of calculation errors even for the "valid area". For planar sensing, this error can be estimated from knowledge of the measured data at the edge of the sensing area, even though the error arises from neglecting all data on an infinite plane outside the sensing area. For a preliminary estimation of the error due to the limited sensing area for measurements on a planar area, the following applies:

$$\frac{|\Delta I(\mathbf{K})|}{|I(\mathbf{K})|} \leq \frac{\alpha \lambda L_m b_m(\rho', \varphi_\rho)}{2S \cos\gamma_m} \frac{|I(\mathbf{K}_0)|}{|I(\mathbf{K})|} \quad (11)$$

Where:
S is the area of the antenna aperture, Lm is the maximum width of the sensing area,
$\alpha \approx 1 - 5$ is the amplitude drop coefficient (1 for uniform irradiance, but practically no more than 4 for commonly used irradiance), $b_m(\rho', \varphi_\rho)$ is the maximum amplitude of the probe output at the edge of the sensing area relative to the maximum probe output at the sensing area, and $|I(\mathbf{K}_0)/I(\mathbf{K})|$ is the ratio of the maximum amplitude in the $\mathbf{K}_0$ direction to the amplitude in the K direction (i.e. The inverted value of the normalised diagram in the far zone). As an upper bound, (11) holds for angles up to 90°, but very roughly, equation (11) can be said to represent a fairly reasonable estimate of the upper error for a range of angles less than Φ/2, and for larger angles the estimate of (11) is much higher than the actual errors.

That relationship requires less information, but generally gives a much larger upper bound on the error. This relationship can be applied even for antennas that are separable in the x,y plane only when scanning along the antenna axes, as has been shown not only theoretically but also experimentally. However, it should be noted that the above relation does not consider the phase change along the perimeter of the sensing area when measuring

ISSN 2669-0195 (online) http://jssidoi.org/jesi/
2022 Volume 4 Number 1 (March)
http://doi.org/10.9770/IRD.2022.4.1(7)

along the antenna axes and therefore could give larger errors in most cases. Therefore, it can be assumed that this relation for planar sensing can be used as an upper estimate for cylindrical sensing as well.

3. Experimental results of error analysis

In the next part of the paper we present examples of measurements, comparison of measurements on the cylindrical surface and in the far zone, numerical simulation of errors that occur during measurements and statistical processing of 10 measurements for cylindrical measurements (one slice) for a probe consisting of both a shortened dipole and an open reduced rectangular waveguide. A comparison of the statistical processing of the measurements and estimates of the effect of random errors is shown, considering a suitable error correlation interval. The maximum values of the standard deviations of the σ ten measurements for wavelength λ = 32 mm were approximately 0.02 (0.2 dB for gain). However, it is important to note that this figure refers to the total errors due to both the effect of the sensing mechanism (which were quite significant due to inaccurate manual positioning and a not very rigid sensing mechanism), as well as the errors of all instruments used (amplitude errors due to receiver non-linearity and source amplitude instability with maximum standard deviations σ_φ estimated at 0.01 and phase errors due to phase changes in the microwave path including rotary couplers). The resulting standard deviations of σ_φ all phase errors were estimated to be 0.02 (in the middle of the sensing interval) to 0.1 (at the edges of the sensing interval). Error estimation was performed using backward FFT from the measured error spectra (which was obtained using FFT from the measured values). Numerical simulations were performed for different error variations. In particular, the influence of the type of correlation function, the correlation interval used and the shape of the measured amplitude and phase were studied. The use of numerical simulations allowed investigating much more complex shapes of amplitudes and phases as well as various types of correlation functions and random processes. This of course on the one hand leads to much more realistic estimates that are in better agreement with experimental data, but on the other hand this approach is more limited to special types of errors and therefore does not give an idea of the potential for much larger errors in some special cases (the analysis is instead focused on somewhat exceptional cases where special error distributions produce the largest possible errors). For testing, errors were created by incorrect alignment of the sensing mechanism on the straight line and the rotation axis of the measured antenna. The base of the tower was tilted to form a known angular tilt between the z-axis of rotation and the scan axis. This is a typical positional error that can occur in cylindrical measurements. The tower was rotated by 0.1° and measurements made. Comparison of the characteristics in the far zone without and with the above error gives directly the magnitude of the effect for this special type of error. The tilt of the tower causes a maximum radius error of 1.12 mm and a standard deviation of 0.76 mm. Equation (3) gives an error estimate of 0.05 dB and the change in measured gain was 0.052 dB.

Therefore, for the investigation, a known error was inserted into the radius size to obtain the sensitivity of the radiation pattern in the far zone. The measured antenna was mounted on a rotating device that was mounted on an automatic sliding device that allowed the radius to be changed. The measured X-band antenna with sum and difference beam was first measured using planar scanning to obtain a reference radiation pattern. Then cylindrical scanning was used with a scanning range of 100° (0.5° rotation step) and a vertical probe movement of 2 m (16.5 mm step). The radius size (distance of the probe from the axis of rotation of the measured antenna) was set to 1.1 m. To test the device for measurements on a cylindrical surface, the radius deflection was set to 0, -0,2 λ, -0,4 λ , .. -1,6 λ. These data were processed so that the radius size was considered to be the same (1.1 m) for all cases, which caused a processing error because the radius actually varied. The results are shown in Figures 1,2,3,4.

INSIGHTS INTO REGIONAL DEVELOPMENT
ISSN 2669-0195 (online) http://jssidoi.org/jesi/
2022 Volume 4 Number 1 (March)
http://doi.org/10.9770/IRD.2022.4.1(7)

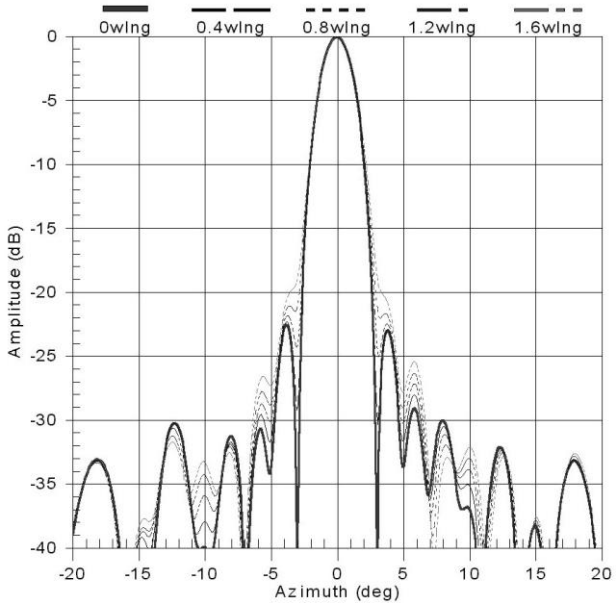

Figure 1. Radius change of 0, -0,4 λ, -0,8 λ , -1,2 λ and -1,6 λ for the sum beam in azimuth

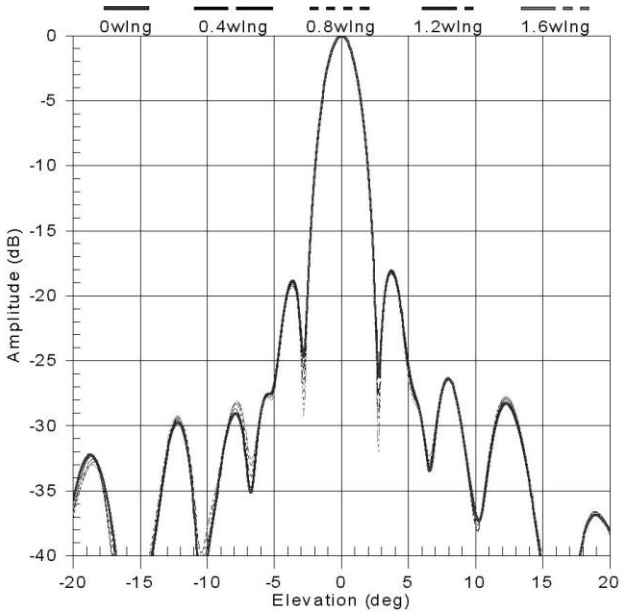

Figure 2. Radius change of 0, -0.4λ, -0.8λ, -1.2λ and -1.6λ for the summed beam in elevation

ISSN 2669-0195 (online) http://jssidoi.org/jesi/
2022 Volume 4 Number 1 (March)
http://doi.org/10.9770/IRD.2022.4.1(7)

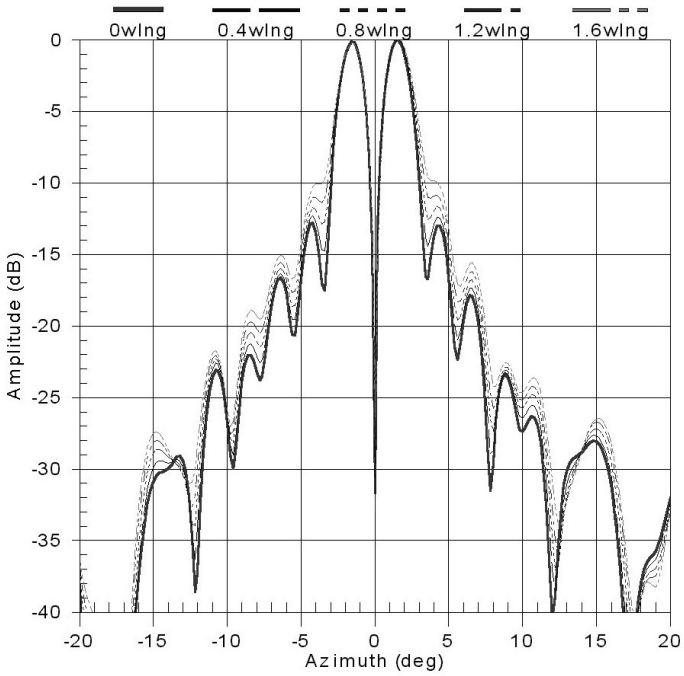

Figure 3. Radius change of 0, -0.4λ , -0.8λ, -1.2λ and -1.6λ for the difference beam in elevation

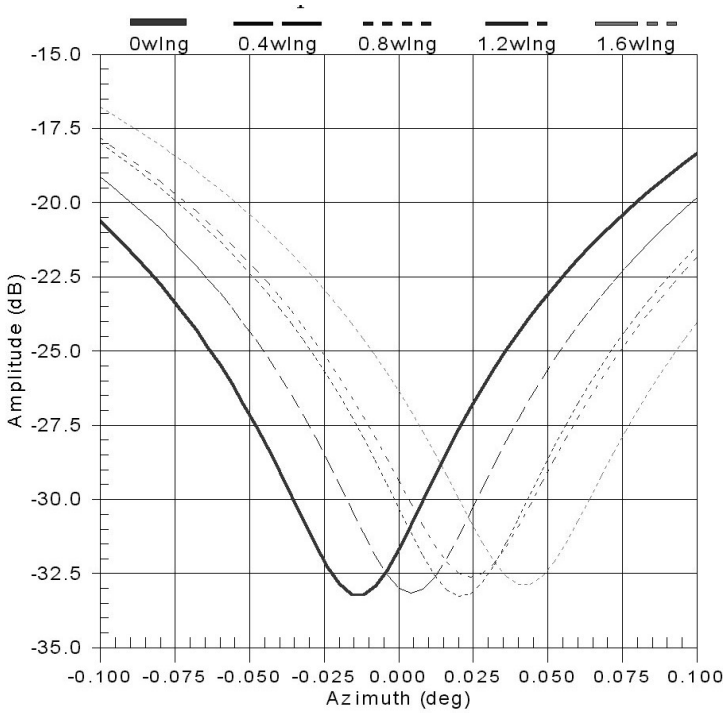

Figure 4. Radius change by 0, -0.4λ, -0.8λ, -1.2λ and -1.6λ for the summation beam in elevation (detailed waveform near zero)

ISSN 2669-0195 (online) http://jssidoi.org/jesi/
2022 Volume 4 Number 1 (March)
http://doi.org/10.9770/IRD.2022.4.1(7)

The azimuthal characteristics varied slightly, as demonstrated by the comparison of individual characteristics in Figure 1. A change in radius of -0.4λ corresponds to the 0.4wlng designation, and similarly for the other values in Figs. 1 to 4. The elevation beam characteristics were found to be relatively insensitive (hardly changed), as demonstrated by the comparison of the individual characteristics in Fig.2. Comparison of the difference beam revealed similar behavior for the azimuthal and elevation characteristics. However, for the azimuthal characteristic, a more significant change in zero position was found for the difference beam (0.05°), as demonstrated by the comparison of the individual characteristics in Figures 3 and 4. It can be summarized that the effect of the change in radius is almost negligible for the elevation beam characteristic and is more significant for the azimuthal characteristic. The measured data showed a preliminary conclusion that the target accuracy for radius determination must be better than 0.1λ. This is less stringent than usually considered. However, due to the change in the position of the zero of the difference beam in the azimuthal characteristic, further investigation would be advisable.

In the next experiment, data were measured along the antenna axes at a distance of 25 cm from a circular array with a diameter of 80 cm. The sensing range was 213 cm and this range was gradually reduced. The wavelength used was 3.26 cm. A similar experiment was performed for a reflector antenna with a frequency of 60 GHz. Comparisons showed that the conclusions presented for the limited sensing area analysis were valid. Of course, these experiments were performed for "planar sensing" (along the antenna axes). Since these experiments were performed only for the axes, it can be assumed that even smaller errors will arise when scanning on a cylindrical surface (this will be an "average" value over all scans). Since these errors will usually be very small, it is probably not necessary to find better estimates of the errors.

In Table 1, the errors calculated from relation (11) are given for some parameters of the calculated radiation characteristics in the far zone of a typical antenna operating in the X-band with sum and difference beam. Wavelength = λ0.0326 m¸ aperture area S = 0.5 m2, maximum scanning area width Lm =1.6 m, λ= 3, maximum angle λ= 60°, amplitude drop at the edge of the scanning area -45 dB. The sidelobe level was -25 dB, the "zero" level of the differential beam was -30 dB.

Table 1. Calculated errors

	Radiation characteristic parameter	Errors due to final scanning
Sum bundle	Maximum axis gain	**±0,01 dB**
	Level of the lateral lobes	**±0,16 dB**
	Bundle width ϕ_0	**±0,002 ϕ_0**
	Polarization ratio on axis	**±0,001**
Differential bundle	The value of "zero"	**±0,28 dB**
	Shift "zero"	Negligible
	Main volumes	**±0,01 dB**

ISSN 2669-0195 (online) http://jssidoi.org/jesi/
2022 Volume 4 Number 1 (March)
http://doi.org/10.9770/IRD.2022.4.1(7)

Conclusions

Thus, it can be summarized that for accurate measurements in the near zone, the sensing device should have a probe positioning accuracy of the order of one hundredth of a wavelength for the highest frequency considered. Except for very special error waveforms, a standard deviation value of approximately λ/100 is usually sufficient (errors greater than three times the standard deviation will occur with a probability of approximately one per mil).

Since antennas with smaller aperture sizes can be expected to be used for the highest frequencies, it is possible to design a smaller sensing device with higher accuracy or to ensure that the central part of the sensing device has higher accuracy. Another possibility is to accurately measure the errors of a stable sensing device and correct the errors in the z-direction using special software, or to better adjust the sensing device or refine the error estimates and confirm that the device can be used. Similarly, it is possible to estimate the magnitude of δ_{φ}. Since the average error δ_y (φ) is equal to one half of the value in equation (7), δ_y (φ) = π D_x δ_{φ} /180 and therefore $\delta_{\varphi}=0{,}57\lambda/D_x$. If we consider that usually the dimension

Dx will be less than 30 λ, then it δ_{φ} should be about 0.02° (which, except in special cases, may not be the maximum error but rather the standard deviation). Note that different manufacturers specify roughly the same values.

References

Aghjian, A. D. 1975. Upper-bound errors in far-field antenna parameters determined from planar near-field measurements. Part 1: Analysis. National Bureau of Standards, Ernest Ambler https://doi.org/10.6028/NBS.TN.667

Aghjian, A. D. 1977. Near-field antenna measurements on a cylindrical surface: A source scattering-matrix formulation. National Bureau of Standards Technical Note 696. Boulder. https://doi.org/10.6028/NBS.TN.696r

Bayuk, J.L. 2021. Systems Security Engineering, 9(2), *IEEE Security & Privacy*, 72-74 http://doi.org/10.1109/MSP.2011.41

Buday, A., Grinchuk, A., Gromyko, A. 2017. Practical implementation of hardware and software complex for planar measurements of antenna characteristics in the near zone. *Devices and Methods of Measurements*, 8(4), 334-343. http://doi.org/10.21122/2220-9506-2017-8-4-17-23

Chejbal, V. Kovarik, V. 1981. Accuracy of near-field antenna measurement using holography.*Tesla Electronics*, 14(2), 48-52.

Chou, H.T., Gao, W.J., Zhou, J.H., You, B.Q., He, X.H. 2021. Enhancing Electromagnetic Backscattering Responses for Target Detection in the Near Zone of Near-Field-Focused Phased Array Antennas. *IEEE Trans. Antennas Prop.*, 69(3), 1658-1669. https://doi.org/10.1109/TAP.2020.3026878

Epjar, A. G., Newell, A. C., Francis, M. H. 1988. Accurate determination of planar near-field correction parameters for linearly polarized probes. *IEEE Trans. Antennas Prop*., 36(6), 855-768. https://doi.org/10.1109/8.1189

Ivanka, J., Chuda, H. 2015. Theory of near-zone measurement with transformation to aerial surface and gain measurement. *Journal of Electrical Engineering-Elektrotechnicky Casopis*, 66(2), 85-90. http://doi.org/10.1515/jee-2015-0013

Just, J. 1981. Measurement of antennas in the near zone. FEE CTU Prague

Newell, A. C., Lee, D. 2000. Application of the NIST 18 term errormodel to cylindrical near-filed field measurements. Antenna Measurement Techniques Association Conference, Oct. 2000.

Newell, C. 1988. Error analysis techniques for planar near-field measurements. *IEEE Transactions on Antennas and Propagation*, 36(6), 754-768. https://doi.org/10.1109/8.1177

OHDE Schwarz, corporate materials, Test Measurement Produkt, Catalog 2007/2008

Prabhakaran, S., Selvadurai, K. 2018. Performance Analysis of Security Requirements Engineering Framework by Measuring the Vulnerabilities. *International Arab Journal of Information Technology*, 15(3). 435-444.

Rensburg, Daniël Janse van, Newell, A.C., Hagenbeek, M. 2000. The impact of alignment errors on cylindrical near-field antenna measurements. Antenna Measurement Techniques Association Conference, Oct. 2000.

Funding: This research was partly supported by the project, which has received funding from the European Union's Horizon 2020 research and innovation programme European Research Council (ERC) under the European Union's Horizon 2020 research and innovation programme Marie Sklodowska-Curie Research and Innovation Staff Exchanges ES H2020-MSCA-RISE-2014 CLUSDEVMED (2015-2019) Grant Agreement Number 645730730.

Data Availability Statement: All data is provided in full in the results section of this paper.

Author Contributions: Conceptualization: *J.I., V.O.*; methodology: *J.I., V.O.*; data analysis: *J.I., V.O.*, writing—original draft preparation: *J.I., V.O.*, writing; review and editing: *J.I., V.O.*; visualization: *J.I., V.O.*. All authors have read and agreed to the published version of the manuscript.

Jan IVANKA (Ing) was born in Puchov, Slovak Republic in 1960. He received the Master degree in Military Communication and Connection Technology at the Military Academy of Technology in Brno, Czech Republic in 1984. He has joined the Department of Security Engineering at the Bata University in Zlin since 2003. His main research interests include aspectsof electromagnetic interference issues and the electromagnetic susceptibility of mechatronic systems and other activities arefocused on software issues designed to determine the time ofdeath of biological materiál in the algor and rigor mortis processes.
ORCID ID: orcid.org/0000-0002-3715-7138

Vladimira OSADSKÁ (Ing., Ph.D.) was born in 1988 in Dolny Kubin, Slovakia. She received her engineering degree in Security Engineering from the VŠB - Technical University in Ostrava, Czech Republic, in 2015 and her Ph.D. degree from the same university in 2018. Since 2019, she has been working as a researcher at the Department of Security Services at VŠB - TU Ostrava. Her main research interests include security systems, system susceptibility to electromagnetic fields as well as security risk analysis.
ORCID ID: orcid.org/ 0000-0002-5417-9240